JOURNAL OF OPTOELECTRONICS AND ADVANCED MATERIALS Vol. 9, No. 1, January 2007, p. 24 - 29

Invited Lecture

Nanosized magnetite for biomedical applications

I. NEDKOV
Institute of Electronics, Bulgarian Academy of Sciences, 72 Tzarigradsko Chaussee, 1784 Sofia, Bulgaria

Nanosized magnetite particles can be potentially used in the targeted delivery of therapeutic agents *in vivo*, in the hyperthermic treatment of tumours, in magnetic resonance imaging (MRI) as contrast agents and in the bio magnetic separation of bio-molecules. An understanding of the motion, heating and visualization of these nanoparticles in physiological systems *in vitro* and *in vivo* is required to tailor these nanoparticles for some of these applications. These applications are based on the biocompatibility of magnetite and on the nanoparticle's magnetic characteristics, namely the superparamagnetic (SPM) behaviour and the high saturation magnetization (magnetite exhibits one of the largest magnetic moments among oxides). The very small crystal size and the surface effects have a strong influence on the magnetic behaviour of these materials. The work sets out to clarify the impact of oxidation on the magnetite particle characteristics and presents new data about some bio-magnetic applications for SPM magnetite.

(Received November 1, 2006; accepted December 21, 2006)

Keywords: Magnetite, Nanoparticles, Surface effects, Hyperthermia

1. Introduction

Nanostructured magnetite was one of the first ferroxide materials with proven vital functions in the bio-world. The bio-origin (the so called bio-mineralization of ferromagnetic materials) of a large part of the magnetite on the Earth's surface was one of the first proofs for the existence of living organisms on our planet [1,2]. In 1960 [3], the development of the first magnetic nanoparticles based on a stable magnetic fluid (ferrofluids) and the development of nanotechnologies provoked new hopes for medical applications, such as targeted drug delivery *in vivo*, contrast agents in magnetic resonance imaging (MRI) tomography, the bio-magnetic separation of DNA and proteins, hyperthermia, etc. These applications are based on the biocompatibility of magnetite and on the nanoparticle's magnetic characteristics, namely, superparamagnetic behaviour and a high saturation magnetization (magnetite exhibits one of the largest magnetic moments among oxides). An important characteristic, in view of possible bio-applications, is the particle's total magnetic moment. The existence is well known in nanoparticles of the so-called "boundary effect" which leads to a decrease in the particles' magnetization in comparison with that of bulk magnetite [4]. This is why comprehensive studies are necessary of the particle's surface and its contribution to its overall magnetic behaviour. The particles' super-paramagnetic properties at temperatures typical for vital processes is the first necessary condition for the applications discussed, since they determine the manifestation of the particles' magnetic behaviour only in the presence of an external magnetic field. When the particle size reaches a critical threshold, where the remnant magnetization and the coercive force tend to zero, the particles become superparamagnetic (SPM). A mono-domain particle with volume V possesses a permanent magnetization directed along the easy magnetization axis. If the volume V is sufficiently small, or the temperature is high enough, the thermal energy (k_BT) becomes sufficient to overcome the energy of anisotropy that separates the (+) and (-) magnetization states and causes a spontaneous change of the magnetization. For SPM particles, the total magnetic moment in the absence of an external magnetic field and at $T>0$ K is 0. When an external magnetic field is applied, one observes alignment of the magnetic moments. The magnetic state of such particles is similar to the paramagnetic state, with the exception that in SPM particles the magnetic moment is a collective effect due to all atoms in a particle, rather than of a single atom (as in paramagnetism). In a super-paramagnetic state, therefore, one observes a much higher value of the magnetic susceptibility in comparison to the paramagnetic state. Since the SPM particles exhibit magnetic properties only in the presence of a magnetic field, in bio fluids they can be removed from a suspension by applying a magnetic field and it is easy to re-disperse it in a homogeneous mixture in the absence of a magnetic field. As a result of variations of the applied field or of the temperature, an SPM particle reaches an equilibrium magnetization value after a characteristic relaxation time. The relaxation processes in mono-domain particles take place via two different mechanisms. In the case of ferrofluids, the first one is due to the Brownian motion. The second one corresponds to rotation of the magnetization vector, if one ignores the Brownian motion and considers a motionless particle. It is known as Néel relaxation [5] for monodomain magnetic particles. The relaxation time for Brownian motion is [6]:

$$\tau_B = \frac{4\pi\eta r^3}{k_B T} \quad (1)$$

while the Néel relaxation is [5]:

$$\tau_N = \tau_0 \exp\frac{KV}{k_B T}, \quad (2)$$

where η is the viscosity of the liquid, r is the hydrodynamic radius of the particle, k_B is Boltzmann's constant, τ_0 is a time constant, $\tau_0 \sim 10^{-9}$ s and K the anisotropy constant, and V is the particle volume. When an external *ac* magnetic field supplies energy, it assists the magnetic moments in overcoming the energy barrier, and the energy could dissipate when the particle moment relaxes to its equilibrium orientation. The losses caused by the Néel relaxation lead to heating of the particle ensemble, i.e., the so-called effect of hyperthermia is manifested, and the fluid heats up [7]. Experiments on animals have shown that hyperthermia is a promising technique for treating tumour formations [8,9,10]. Considering the relaxation time as a function of V and T makes it possible to define a blocking temperature - T_B, (at V=*const*) or V_B (at T=*const*), where the magnetization passes from an unstable state (τ<<t) to a stable one (τ>>t).

The aim of this work is to present a complete cycle of studies on nanosized spherical magnetite particles and on hybrid particles – the magnetite/polymer envelope. We will also discuss the possible biomedical applications of a ferrofluid based on such particles.

2. Experimental

Two different technologies [11] for Fe_3O_4 powder preparation with different particle sizes were applied. In the first, strongly diluted solutions of $FeCl_2.4H_2O$ were used (0.03M) – main solutions, and $NaNO_2$ (0.02 M) – oxidizing solution with distilled water. The partial oxidation of Fe^{2+} to Fe^{3+} was carried out by mixing the two solutions in a strict volume ratio, and the co-precipitation by adding a NaOH (0.3 M) solution. This was followed by decantation, filtration, washing to pH=7, and drying at 50 ^oC. In the second one, strongly diluted solutions were prepared of $FeCl_2.4H_2O$ (0.03M) with $FeCl_3.6H_2O$ (0.03 M) with distilled water. The two main solutions of Fe^{2+} and Fe^{3+} were mixed in a ratio of 1:2 and the co-precipitation process was performed by adding an alkaline solution of NaOH (0.3 M) to the mixture. The processes were described in detail in [12].

The preparation of the ferrofluid started with the synthesis of magnetite nanoparticles with two different average sizes following a soft chemical technology, by means of co-precipitation of Fe^{2+} and Fe^{3+} cations in an alkaline medium at room temperature. The black precipitate was washed by distilled water five times, to pH = 7. After washing the magnetite, the wet precipitate (with a fixed amount of 100 mg pure Fe_3O_4 in it) was mixed with 1 ml surfactant – tetramethylammonium hydroxide - $N(CH_3)_4OH$- and then homogenized by intensive stirring. A much larger quantity of dry β-cyclodextrin, needed for preparing a saturated solution, was then added to the mixture, followed by dilution to 100 ml with distilled water. The ferrofluid thus obtained was heated to 50 ^oC and stirred for 20 min. The experiment was conducted at atmospheric pressure and room temperature.

The XRD data exhibited consistently a single-phase spinel structure for the samples examined. The TEM bright-field images and the grain-size statistics of the powders obtained were also analyzed. The samples obtained were investigated by IR-spectroscopy in the 4000-400 cm^{-1} region, using the KBr pellet technique (Nicolet-320 FTIR spectrometer). The Mössbauer spectra were taken with an electromechanical spectrometer working in a constant acceleration mode. A 70 mC $^{57}Co(Cr)$ source and an α-Fe standard were used. The particle surface was investigated by means of integrated low-energy electron Mössbauer spectroscopy (ILEEMS) following the methodology described in [13]. The experimentally obtained spectra were computer-fitted to a series of Lorentzian curves by the least-squares method. The high-field magnetization measurements, up to 60 kOe, were carried out using a SQUID magnetometer.

Heating experiments were performed in a simple arrangement using a coil with three windings. The *ac* field was generated by means of a home-made generator with a power of 10 kW (40 kHz). The temperature was measured by Cu-Constantan thermocouples placed at different distances from the heating source.

3. Results and discussions

3.1. Nanostructured magnetite

We studied selected groups of nanostructured powders with various average particle sizes (from 5 nm to 300 nm) and with a high size homogeneity, for which the XRD data indicated unambiguously a single-phase magnetite. Using IR spectroscopy, we established the presence of maghemite (γ-Fe_2O_3). IR-spectroscopy proved to be a very useful tool for examining the undesirable oxidation towards γ-Fe_2O_3, because of the clear difference in the constant absorption bands for magnetite and maghemite (630 cm^{-1} for γ-Fe_2O_3 and 580 cm^{-1} for Fe_3O_4 [14]). This difference is obvious even for materials on the nanometer scale. Following prolonged exposure to air, the oxidation process in the powders continued (see Fig. 1).

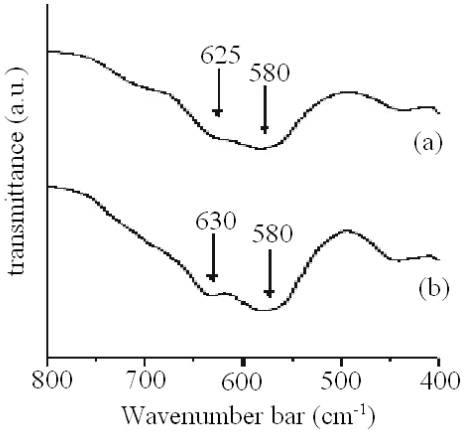

Fig. 1. FTIR spectra of magnetite with a particle size of 10 nm (a) a week after the synthesis, (b) 60 days later.

The Mössbauer spectroscopy (MöS) measurements of the selected powders at room temperature also pointed to the presence of maghemite. Fig. 2 shows spectra for powders with different average particle sizes.

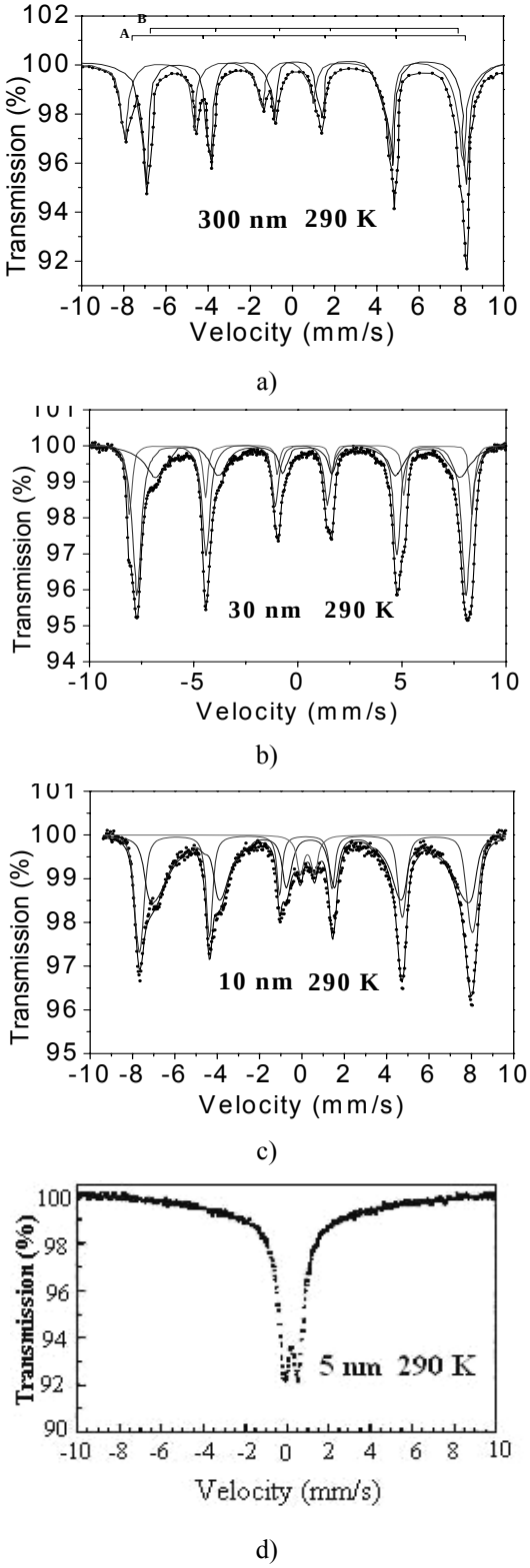

Fig. 2. MöS of magnetite powders with average particle sizes a) 300 nm; b) 30 nm; c) 10 nm and d) 5 nm.

The larger particles with sizes of 300 nm and above exhibit typical magnetite spectra, while reducing the size leads to changes in the spectral structure related to oxidation processes. MöS reveal super-paramagnetic behaviour of the powders with particle sizes of less than 5 nm. The double peak in the spectrum of super-paramagnetic magnetite contradicts the Mørup theory [15] and gives one reason to expect oxidation of the particles' surfaces and changes in the magnetic behaviour due to the increased contribution of the surface via small particles.

The clarification of the processes of oxidation in nanostructured magnetite was deepened by using integrated low-energy electron Mössbauer spectroscopy (ILEEMS), which allows one to examine the particle's surface. Fig. 3 illustrates a typical spectrum of particles with sizes of less than 10 nm.

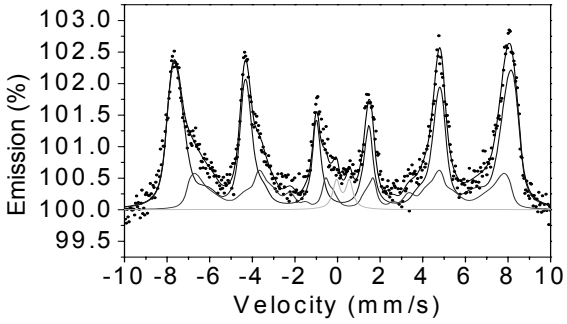

Fig. 3. ILEEMS of the surface of a magnetite particle with size 10 nm.

The analysis of the changes in the surface content of Fe^{3+}/Fe^{2+} in a magnetite particle as a function of its size allowed us to explore the oxidation processes. The latter are expressed in the changes in the Fe^{2+} content in the octahedral sub-lattice of magnetite at the expense of the appearance of cation vacancies. The surface structure approaches that of maghemite (γ-Fe_2O_3). Our experiments showed that the changed surface stoichiometry can be described by the structural formula: $(Fe^{3+})_A[Fe^{3+}_{5x}Fe^{2.5+}_{2-6x}\varphi_x]_BO_4$, where φ denotes vacancies in the octahedral sub lattice. In the samples studied, x varied from 0 to 0.22 but did not reach the value typical for pure maghemite ($x = 0.33$). This is why we refer to this surface as a quasi-maghemite structure.

The ILEEMS demonstrated that these changes in the surface defects occur smoothly from the particle core to its surface, starting from a depth of approximately 3 nm, with the particle core remaining pure magnetite. This depth of oxidation, formed immediately following the powder preparation, is retained regardless of the particle size. The TEM studies of the same powders confirm the ILEEMS data [12].

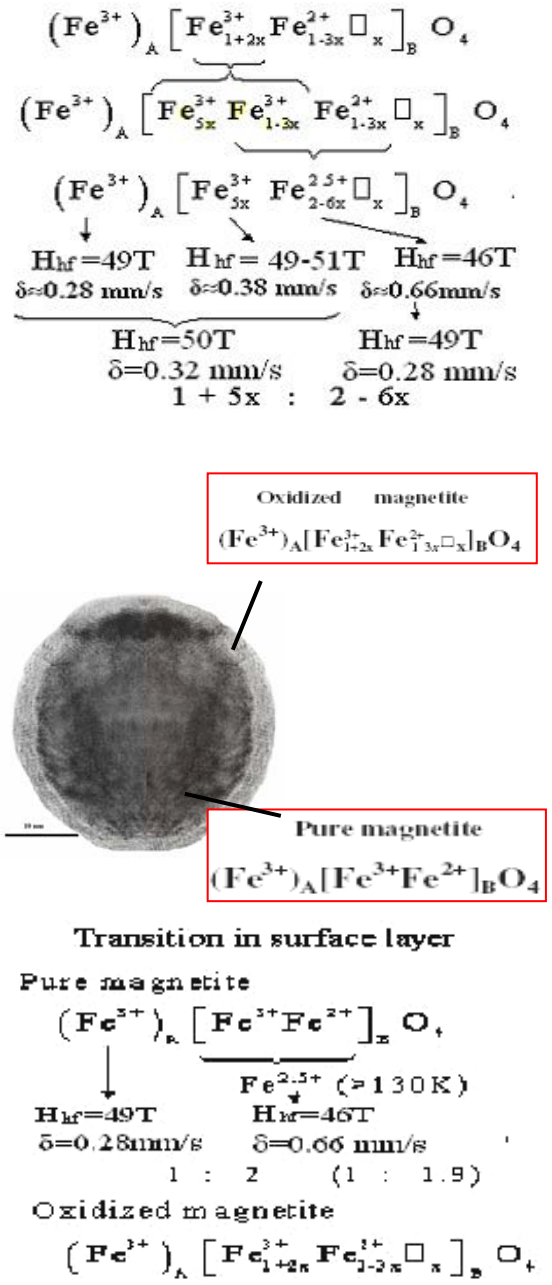

Fig. 4. HRSEM picture of the surface structure of a magnetite particle of size 30 nm and summarized MöS data on the changes in the cation distribution and in ion vacancies in the surface and the core of the particle.

Fig. 4 is an illustration of the changes in the structure observed by means of high-resolution SEM, and also presents summarized ILEEMS and transmission MöS data on the surface and core of a magnetite particle of size 30 nm. One can see from HRSEM that the changes take place to a depth of about 3 nm. The studies explain the changes in the MöS spectra as the particle diameter are reduced, which are obviously related to the increased contribution of the surface, i.e., as the particle size diminishes, the effective surface augments its share and exerts an increasing influence on the nanoparticle's magnetic properties.

Using the Greens' function formalism, one can describe a three dimensional magnetic spherical superparamagnetic particle by two-dimensional interactions within a single shell and between neighbouring shells [16]. The number of shells, N, is an outer parameter, so spherical particles with different sizes could be modelled. This is based on the icosahedron's magic numbers for the magnetic atoms in each shell, known from the physics of clusters and quasi-crystals. Considering the surface effect, an anisotropy term may be included in the energy. It should have different values for the core and for the surface. At each temperature, the energy E_i of each shell is calculated first. This energy calculation is done shell by shell. We would like to clarify this, and in our calculations E_i has the meaning of the energy of the shell per its average magnetization:

$$E_i = g\mu_B H_0 + I_B s_i^z + nJ_B S_i^e + n_{up} J_B S_{i+1}^e + n_{down} J_B S_{i-1}^e \quad (3)$$

We calculate the energy of the whole system shell by shell, as a sum of spin-orbital (s-d model) interactions for the conduction electrons, the Heisenberg term for the exchange interaction between the magnetic atoms, and a term for the energy in a magnetic field. The Heisenberg term has three parts. Each magnetic atom interacts with its nearest neighbours:

- in the current shell (n);
- in the upper shell (n_{up}) and
- in the lower shell (n_{down})

The surface effect is considered in two ways:
by the absence of interaction of the last shell with the upper one, i.e. the symmetry is broken and the number of next-neighbours is reduced; by introducing exchange interaction constants J_S (for magnetic atoms), I_S (for the interaction of the conduction electrons in the s-d model) at the surface, differently from their corresponding values in the core J_B, I_B (the exchange constants for the bulk).

Then, the average magnetization S_i^z of each shell in the mean field approximation (MFA) is calculated. It is a function of the energy of the corresponding shell, the temperature and the spin value S of the magnetic atom:

$$S_i^z = S + 0.5 \coth [S + 0.5\, E_i/k_B T] - 0.5 \coth 0.5\, E_i/k_B T \quad (4)$$

Then, to calculate the energies of the interactions of the *'up'* and *'down'* conduction electrons with magnetic atoms:

$$L_i^{up} = -I_B S_i^z \;;\; L_i^{down} = I_B S_i^z \quad (5)$$

The calculation of the distribution densities d_{up} and d_{down} for "*up*" and "*down*" conduction electrons is the next step:

$$d_{up} = \frac{1}{e^{L_i^{up}/k_B T} + 1} \;;\; d_{down} = \frac{1}{e^{L_i^{down}/k_B T} + 1} \quad (6)$$

The last step of the procedure is the calculation of the average value of the spin s_i^z of the conduction electrons in each shell:

$$s_i^z = \frac{d_{up} - d_{down}}{2} \tag{7}$$

When we complete this procedure, we return to the beginning of the algorithm and calculate the new values of the energy of each shell with the new values of the magnetization S_i^z of the shells and the spins s_i^z of the conduction electrons in the shells. We repeat this procedure until the equilibrium values are reached. Thus, a system of non-linear interconnected equations is solved self-consistently.

The starting point is a fully ordered system at low temperature. By increasing the temperature gradually, one can simulate the demagnetization process. The temperature at which a particle becomes fully demagnetized - the Curie temperature - could be calculated by the described model. Thus, the demagnetizing behaviour of the whole particle could be monitored shell by shell. The model makes it possible also to simulate the magnetic behaviour of the particle in an applied magnetic field (constant and oscillating) at different temperatures. Thus, one can produce hysteresis curves, which are a basic characteristic for a magnetic state of the magnetic nanoparticle for temperatures up to the blocking temperature. Demagnetization starts from the surface to the core when $J_S < J_B$. This result is important from a fundamental point of view, because it shows the role of the surface in two completely different directions. Thus, it is a clue for understanding the prime cause of the peculiar behaviour of the nanoparticle.

3.2. Hybrid nanostructured particles– magnetite/polymer envelope

Our further research was focused on the preparation of hybrid particles – magnetite/polymer envelopes with the aim of developing bio-active fluids for medical applications. A well-developed technology for producing nanosized magnetite (Fe_3O_4) was used for the synthesis of a novel type of biocompatible nanosized magnetic core/shell structure. Numerous investigations by means of FTIR-spectroscopy, XRD and MöS were made in order to follow the development of undesirable oxidation on the surface of the magnetite particles towards maghemite (γ-Fe_2O_3) [12]. These investigations allowed us to use a magnetite phase with average particle diameters of 5±2 nm, which were used to form a stable colloidal ferrofluid.

The organic material was β-cyclodextrin, which is widely used in the pharmaceutical industry due to its unique structure and properties. Beta-cyclodextrin is a cyclic, water-soluble, non-reducing oligosaccharide, built up from seven glucopyranose units and containing 21 hydroxyl groups of which the primary ones (seven) are the most reactive and capable of establishing weak hydrogen bonds [17]. Fig. 5 presents SQUID data on the changes in the magnetic properties of magnetite particles, and of hybrid particles of the same size. The MöS (Fig. 5c) and temperature dependent magnetization in the zero-field-cooled (ZFC) and field-cooled (FC) states at 100 Oe (Fig. 5b) measurements demonstrated that the coated particles are also SPM at room temperature (RT), and for the hybrid particle the magnetization (Fig. 5a) at RT is lower by about 15 % than of the non-encapsulated particle. The IR spectroscopy data (see Fig. 6), as observed for the coated particles, coincides with the absorption band at 580 cm^{-1} characteristic for magnetite and does not exhibit a split in the spectra, meaning that the oxidation on the surface of the particles is avoided.

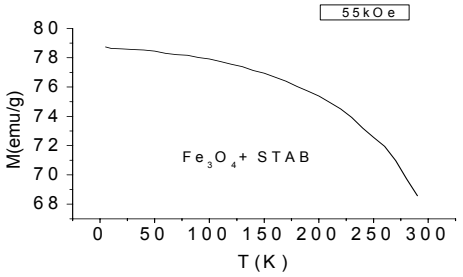

a)

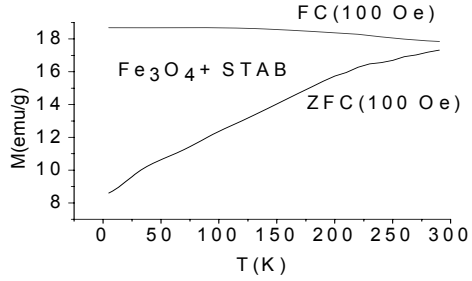

b)

c)

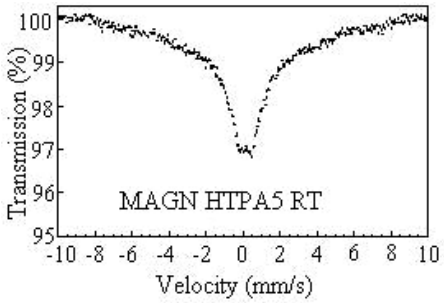

Fig. 5. Temperature dependence of magnetization and FC and ZFC magnetization curves for a) Fe_3O_4 with particle size 5±2 nm and b) hybrid Fe_3O_4 with CTAB and β-CD of particle size 12 ± 5 nm and c) MöS of a hybrid particle.

No transition towards maghemite is indicated by the spectra obtained. All characteristic absorption bands for the organic agent are present (1040, 1170, 3420 cm^{-1} etc.), providing a proof that the cyclic character of the cyclodextrin molecule is retained. This fact is essential in order to apply this unique structure for medical applications.

The studies described above allowed us to carry out an experiment on the possibility for bio-medical applications of the fluid obtained. The effect of hyperthermia at 40 KHz was studied for ferrofluids with SPM magnetite particles. The data obtained (see Fig. 7) confirm the possibility of a temperature increase due to electromagnetic radiation.

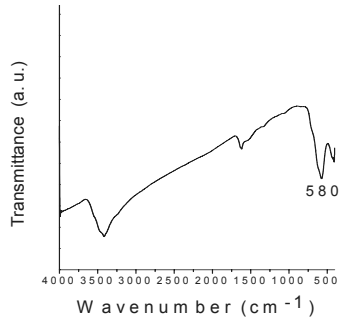

Fig.6. FTIR spectra of the dried magnetite/TMAH/β-CD ferrofluid

The specific absorption rate (SAR) can be calculated from the experimental curve, using the relation SAR = C ($\Delta T/\Delta t$) [18], where C is the sample specific heat capacity, which is calculated as a mass-weighted mean value of the magnetite. The first step was to verify that the electromagnetic field applied did not affect the temperature of a solution free of magnetic nanoparticles. For magnetite, the specific heat capacity is Cmag = 0.937 J/g K, whereas $\Delta T/\Delta t$ is the initial slope of the time-dependent temperature curve. The SAR values of the SPM sample were calculated as about 3.47 W/g. The results show that the ferrofluid containing SPM magnetite particles covered with β-cyclodextrin can be successfully used in experiments related to hyperthermia.

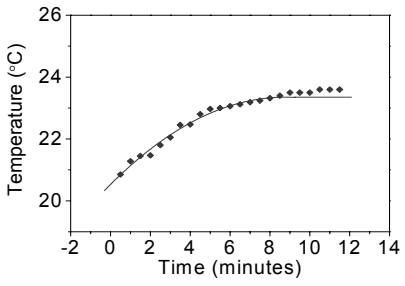

Fig. 7. Hyperthermia effect for a ferrofluid containing Fe_3O_4 nanoparticles enveloped with β-CD.

4. Conclusions

The surfaces of nanostructured spherical particles with diameters below 10 nm, prepared by a soft-chemistry method are oxidized, so that defective spinels with octahedral vacancies are formed.

The oxidation occurs to a depth of approximately 3 nm, and the surface has a quasi-maghemite structure.

The strongly defective surface of a spherical particle can be considered as being a second magnetic phase, since it affects the particle's magnetic properties.

A biocompatible, highly saturated water-based ferrofluid, with long time stability, is synthesised using magnetite with an average grain size of 5 nm, coated with a widely applicable (in the pharmaceutical industry) substance, namely β-cyclodextrin.

The effects of hyperthermia were observed for the ferrofluid based on super-paramagnetic magnetite.

Acknowledgements

The work was supported by the Bulgarian National Council for Scientific Research, under contract TH-1/01. The author wishes to thank Prof. R.E. Vandenberghe from the Dept. of Subatomic and Radiation Physics, University of Gent, Belgium.

References

[1] D. Schuler, ESF Intern. Conf. Nanoscale Magnetic Oxides and Bio-World, Ed. I. Nedkov and Ph. Tailhades, Heron Press. 234 (2004).
[2] H. Dong, Chemical Geology, 299 (2000).
[3] R. E. Rosensweig, Scientific American **247**, 136 (1982).
[4] R. H. Kodama, A. E. Berkowitz, Phys. Rev. **B 59**, 6321 (1999).
[5] L. Néel, Ann. Geophys. **5**, 99 (1949).
[6] I. Hrianca, I. Mălăescu, JMMM. **150,** 131 (1995).
[7] R. Hergt, W. Andrea, C. G. d'Ambly, I. Hilger, W. A. Kaiser, U. Richter, H-G. Schmidt, IEEE Trans. Magn. **34**, 3745 (1998).
[8] K. Yagi, Y. Hayashi, N. Ishida, M. Ohbayashi, M. Mizuno, J. Yoshida, Biochem. Mol. Biol. Int. **32**, 167 (1994).
[9] B. Le, M. Shinkai, T. Kitade, H. Honda, J. Yoshida, T. Wakabayashi, T. Kobayashi, J. Chem. Eng. Jpn. **34**, 66 (2001).
[10] D. Bahadur, Jyotsnendu Giri, Biomaterials and magnetism **28**, 639 (2003).
[11] Bulgarian patent BG No 107837 / 22.05.2003/.
[12] I. Nedkov, T. Merodiiska, L. Slavov, R. E. Vandenberghe, Y. Kusano, J. Takada, JMMM. **300**, 358 (2006).
[13] R. E. Vandenberghe, T. Becze-Deak, E. De Grave, ICAME-95, Conference Proceedings, Ed. I. Ortalli (1996).
[14] G. W. Poling, J. of Electrochem. Soc. **116**, 7 (1968).
[15] S. Mørup, M.B. Madsen, J. Frank, J. Villadsen, C. J. W. Koch, JMMM. **40,** 163 (1983).
[16] E. Daykova, Scientific Report, Modeling of superparamagnetic iron oxide nanoparticles, Inst. Electronics BAS (2006).
[17] Cyclodextrins and their inclusion complexes, Ed. J. Szejtly, Akademiai Kiado, Budapest (1982).
[18] M. Babincova, D. Leszczynska, P. Sourivong, J. Magn. Magn. Mater. **225**, 109 (2001).

*Corresponding author: nedkov@ie.bas.bg